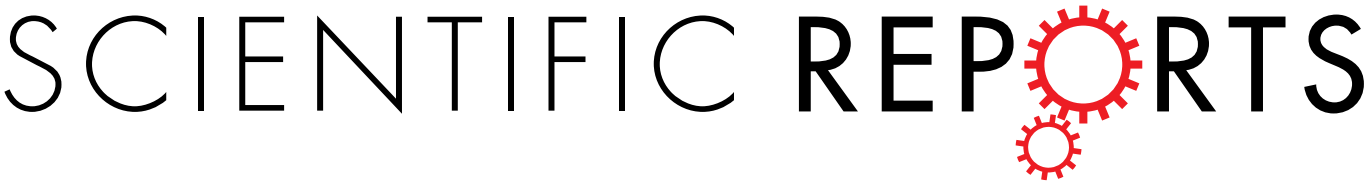

OPEN

Exploring corrections to the Optomechanical Hamiltonian

Kamila Sala & Tommaso Tufarelli

Received: 6 March 2018
Accepted: 16 May 2018
Published online: 14 June 2018

We compare two approaches for deriving corrections to the "linear model" of cavity optomechanics, in order to describe effects that are beyond first order in the radiation pressure coupling. In the regime where the mechanical frequency is much lower than the cavity one, we compare: (I) a widely used phenomenological Hamiltonian conserving the photon number; (II) a two-mode truncation of C. K. Law's microscopic model, which we take as the "true" system Hamiltonian. While these approaches agree at first order, the latter model does not conserve the photon number, resulting in challenging computations. We find that approach (I) allows for several analytical predictions, and significantly outperforms the linear model in our numerical examples. Yet, we also find that the phenomenological Hamiltonian cannot fully capture all high-order corrections arising from the C. K. Law model.

Cavity quantum optomechanics is a rapidly developing research field exploring the interaction of quantised light with macroscopic mirrors, membranes and levitated nano-objects through radiation pressure[1–4]. The field has recently witnessed impressive experimental progress, including demonstrations of near-ground-state cooling of mechanical oscillators[5] and normal-mode splitting due to phonon-photon interaction[2,6]. Among its many applications, optomechanics is a promising platform to demonstrate nonclassical behaviour in massive objects[7,8], and may provide novel avenues for the coherent manipulation of quantum light[9–12]. Recently it was also suggested that optomechanics may allow for ultra-high precision measurements, for example probing Planck-scale corrections to the canonical commutation relations[13,14].

The simplest optomechanical setup features a single optical cavity mode, whose frequency $\omega(x)$ depends parametrically on the coordinate x (the 'position') of a mechanical oscillator[15]. Perhaps the most notable example is embodied by a Fabry-Perot resonator with one movable mirror – see Fig. 1.

Most experiments to date have explored the weak coupling regime, in which radiation pressure effects are only visible upon strong driving of the cavity, and the system can be described as a pair of coupled harmonic oscillators[1]. Several experimental platforms, however, are now approaching the single-photon strong coupling regime[2–4,16–18] (strong coupling, or SC, for brevity), in which the anharmonic nature of the radiation pressure interaction must be taken into account. Strong coupling occurs when the the coupling rate of a single photon is greater than the typical loss rates of the setup. Such regime features clear departures from classical behaviour[11,16,19], and facilitates the production of nonclassical states in both light and mechanics[20–22]. A further appealing feature of strong coupling optomechanics is that the Hamiltonian can be diagonalized analytically upon linearising the cavity frequency around the origin, as per $\omega(x) \simeq \omega(0) + x\,\omega'(0)$ (equivalently, this may be seen as a first order expansion in the coupling constant). We shall call *linear model* the resulting Hamiltonian, arguably the most widely used modelling tool in SC optomechanics.

Despite the undeniable success of the linear model as a theoretical device, the need is arising to go beyond this approximation. For example, it was noted by Brunelli *et al.*[23] that the linearized optomechanical Hamiltonian is unbounded from below, with (unphysical) negative energies cropping up at very high photon numbers. While this pathology may be seen as somewhat mathematical (see Appendix A), it highlights that the model must be eventually refined, particularly in view of future experiments aiming to achieve ever larger coupling strengths. Even in systems that are far from the SC, the quest for ultra-precise measurements (e.g. those pertaining Planck scale physics)[14], or for the detection of dynamical Casimir effects[24], demand a more accurate Hamiltonian description of quantum optomechanics.

Armed with these motivations, in this paper we explore and compare two different starting points that may be used to go beyond the linear model: (I) a widely used phenomenological Hamiltonian, which conserves the cavity photon number (*phenomenological approach*); (II) a two-mode truncation of C. K. Law's microscopic Hamiltonian

Centre for the Mathematics and Theoretical Physics of Quantum Non-Equilibrium Systems, School of Mathematical Sciences, University of Nottingham, University Park, Nottingham, NG7 2RD, United Kingdom. Correspondence and requests for materials should be addressed to T.T. (email: tommaso.tufarelli@gmail.com)

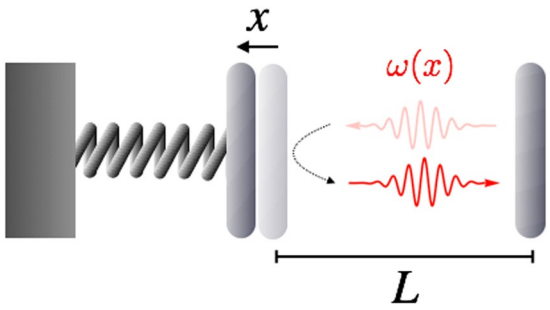

Figure 1. Schematic of an optomechanical Fabry-Perot resonator with one fixed (right) and one movable (left) mirror. Upon reflecting a photon, the movable mirror recoils due to radiation pressure. At the same time the total length of the cavity ($L+x$), hence the photon frequency $\omega(x)$, is modulated by the mirror coordinate x. The movable mirror is subject to a trapping potential (depicted as a spring), which is usually harmonic to a good approximation.

for an optomechanical Fabry-Perot cavity[15] (*microscopic approach*). We shall take this truncated Law Hamiltonian as the benchmark (or "true model") against which the various generalizations of the linear model should be judged. In this paper we focus on the realistic situation where the bare cavity frequency is much larger than the mechanical one. We find that approaches I and II agree at first order in the coupling, but at higher orders the microscopic model yields 'counter-rotating' terms that violate photon number conservation[24] and make computations challenging. We resort to numerical diagonalization of the Hamiltonian, truncated in Fock space, to deal with such situations (and also to tackle the exact phenomenological Hamiltonian). The numerical examples we explored suggest that the phenomenological approach does a good job in improving the linear model in the typical parameter regimes of optomechanics experiments, yet it does not fully capture the second-order corrections arising from the microscopic treatment. We thus conclude that the number-conserving Hamiltonians considered in this paper can provide meaningful refinements to existing optomechanical models, arguably good enough to describe experiments in the near future without adding an excessive computational burden. Yet, our results also highlight that photon-number conservation must be eventually given up to model cavity optomechanics with ultra-high accuracy, even in parameter regimes where dynamical Casimir physics would be usually discounted.

The paper is organised as follows. In Sec. 2 we review the linear model of optomechanics. In Sec. 3 we show how this model can be refined phenomenologically, while in Sec. 4 we discuss model corrections that are microscopically motivated. Sec. 5 features numerical examples comparing the various approaches. We draw our conclusions in Sec. 6, and in Appendix A we discuss in more detail the negative-energies pathology of the linear model[23].

Linear Model: Brief Review

We begin by recalling the model that is commonly taken as a starting point in theoretical optomechanics. To lighten the notation we take $\hbar = 1$, and consider a mechanical mode of unit effective mass. The linear model Hamiltonian reads

$$H_{\rm lin} = (\omega_0 - G\hat{x})\left(\hat{a}^\dagger\hat{a} + \frac{1}{2}\right) + \frac{\hat{p}^2}{2} + \frac{1}{2}\Omega^2\hat{x}^2, \tag{1}$$

where $\hat{a}$ is the annihilation operator for the cavity field mode, $\hat{x}$ and $\hat{p}$ are respectively the canonical position and momentum operators of the movable mirror, Ω is the bare mechanical frequency, ω_0 is the bare cavity frequency, and the coupling constant G is known as frequency pull parameter. The canonical commutators read $[\hat{a}, \hat{a}^\dagger] = 1$, $[\hat{x}, \hat{p}] = i$, while all field operators commute with all mirror operators. In passing we note that the optomechanical interaction strength is often quantified via the vacuum optomechanical coupling strength $g_0 = Gx_{zpf}$, where $x_{zpf} = 1/\sqrt{2\Omega}$ is the position uncertainty in the (bare) ground state of the mechanical oscillator. Loosely speaking, the dimensionless ratio g_0/Ω quantifies the influence a single photon can have on the mirror motion. That being said, many of our expressions will have a more compact form when written in terms of G. We assume that the hierarchy $\omega_0 \gg \Omega \gg g_0$ holds between the model parameters, which is the case in many experimental realizations.

Hamiltonian (1) can be diagonalized exactly[16,20]. The properties of the corresponding eigensystem are well known, and can be obtained from the section: Approach 2: standard quadratic expansion by setting $\beta = 0$.

Phenomenological Approach

A first possibility in extending the linear model, often adopted in the literature, is to consider a phenomenological Hamiltonian similar to Eq. (1), but where the cavity frequency has a more general position dependence $\omega(x)$. Crucially, no change is assumed in the commutation rules for mirror and field operators, an assumption that drastically simplifies computations but may not be justified microscopically[15]–we shall elaborate on this point in the Section: Microscopic approach.

For the purposes of illustration, from now on we consider an optomechanical setup consisting of a Fabry-Perot resonator with one movable mirror (see Fig. 1), which amounts to setting $\omega(x) = \omega_0/(1 + x/L)$ with L the bare cavity length. However, the reader should keep in mind that the same formalism is applicable when $\omega(x)$ is a generic (positive) function. The phenomenological Hamiltonian is

$$H_{\text{phen}} = \omega(\hat{x})\left(\hat{a}^\dagger\hat{a} + \frac{1}{2}\right) + \frac{\hat{p}^2}{2} + \frac{1}{2}\Omega^2\hat{x}^2. \tag{2}$$

If we now pick $L = \omega_0/G = (\omega_0/g_0)x_{zpf}$ and take a first order expansion in G (or equivalently g_0), Eq. (1) is recovered. The natural next step is then to retain higher order corrections in G. In what follows, we discuss two inequivalent approaches that employ simple harmonic oscillator mathematics to approximate Eq. (2) beyond first order. Both methods are in principle amenable to analytical treatment.

Approach 1: photon - controlled harmonic oscillator. Our first approach involves the recalculation of the mechanical equilibrium position and spring constant as functions of the photon number n. Indeed, exploiting the conservation law $[H,\ \hat{a}^\dagger\hat{a}] = 0$, we may decompose

$$H_{\text{phen}} = \sum_{n=0}^{\infty} |n\rangle\langle n| \otimes \left[\frac{\hat{p}^2}{2} + V_n(\hat{x})\right], \tag{3}$$

featuring the effective n-dependent mechanical potential

$$V_n(\hat{x}) \equiv \omega(\hat{x})\left(n + \frac{1}{2}\right) + \frac{1}{2}\Omega^2\hat{x}^2. \tag{4}$$

The idea is now to perform a quadratic expansion of $V_n(\hat{x})$ around its minimum:

$$V_n(\hat{x}) \simeq V_n(\bar{x}_n) + \frac{1}{2}V_n''(\bar{x}_n)(\hat{x} - \bar{x}_n)^2, \tag{5}$$

where the equilibrium position $\bar{x}_n$ is implicitly determined by

$$V_n'(\bar{x}_n) = 0. \tag{6}$$

Note that the above procedure is well defined, since it is easily verified that V_n has a unique global minimum at fixed n, and that for all n, $V_n''(\bar{x}_n) > 0$ (see below). The outlined procedure returns the effective Hamiltonian

$$H_{\hat{n}} \equiv \sum_{n=0}^{\infty} |n\rangle\langle n| \otimes \underbrace{\left(\frac{\hat{p}^2}{2} + \frac{1}{2}\Omega_n^2(\hat{x} - \bar{x}_n)^2 + V_n(\bar{x}_n)\right)}_{H_n}, \tag{7}$$

$$\Omega_n^2 \equiv V_n''(\bar{x}_n), \tag{8}$$

where we have chosen the symbol $H_{\hat{n}}$ to signify that the photon number operator $\hat{n} = \hat{a}^\dagger\hat{a}$ controls which harmonic oscillator Hamiltonian H_n is acting on the mirror. For each n, the eigenvalues and eigenvectors of H_n may be found via straightforward harmonic oscillator techniques. For example the energy eigenvalues, labelled by the cavity photon number n and a mechanical 'phonon' number m (both semipositive integers), read

$$E_{n,m} = V_n(\bar{x}_n) + \Omega_n\left(m + \frac{1}{2}\right). \tag{9}$$

These are all positive, and thus may be used to calculate the partition function without the need for artificial cut-offs[23]. A fully analytical treatment of $H_{\hat{n}}$ requires the explicit inversion of Eq. (6), which may be recast as

$$\Omega^2\bar{x}_n = \left(n + \frac{1}{2}\right)\frac{\omega_0/L}{(1 + \bar{x}_n/L)^2}. \tag{10}$$

This equation for $\bar{x}_n$ is in principle solvable (it is equivalent to a third-degree polynomial equation) but leads to very cumbersome expressions. A number of observations, however, can be made without resorting to the explicit solution. First, it is evident that it must be $\bar{x}_n > 0$, and a little more thought reveals that $\bar{x}_n \to \infty$ when $n \to \infty$. The latter limit is of course a purely mathematical result, indicating that the effective model becomes unreliable when n gets extremely large. Yet, at low photon numbers this model is very accurate at predicting mechanical uncertainties in the energy eigenstates (see Section: Numerical examples). As a second observation, notice that Eq. (10) describes the intersection between a strictly increasing function and a decreasing one, such that for any n there is a unique real solution for $\bar{x}_n$, as anticipated. Third, implicit differentiation in n shows that $\bar{x}_n$ is a strictly increasing function of the photon number (as intution about radiation pressure would suggest). Finally, combining Eqs (8) and (10) the photon-dependent mechanical frequencies may be expressed as

$$\Omega_n^2 = \Omega^2\left[1 + \frac{2\bar{x}_n/L}{(1 + \bar{x}_n/L)}\right], \tag{11}$$

which is a strictly increasing function of $\bar{x}_n$,, hence n. It is an interesting mathematical fact that we obtain the elegant limiting value $\lim_{n\to\infty}\Omega_n = \sqrt{3}\,\Omega$, which does not depend on the cavity parameters ω_0 and L. However,

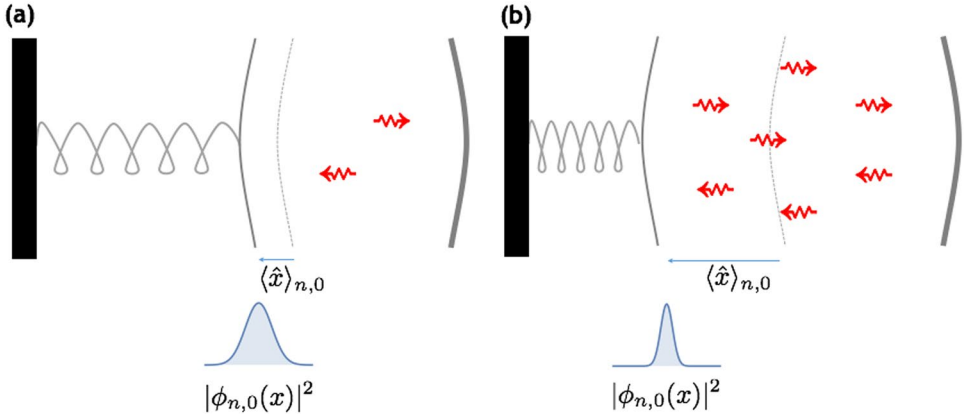

Figure 2. In the two analytically solvable models of the Section: Phenomenological Approach, the optomechanical eigenstates $|\Psi_{n,m}\rangle$ possess a qualitatively similar structure. As the photon number is increased going from (**a**) to (**b**), the average mechanical position is pushed further away from the fixed mirror, while the position uncertainty drecreases (i.e., the mechanical wavefunctions get squeezed). Note that the latter squeezing effect is not present in the linear model.

this result is unlikely to have any physical significance: the above model eventually becomes unreliable when too many photons occupy the cavity (as discussed, the associated limit $\bar{x}_n \to \infty$ means that the average cavity length becomes infinite!). The eigenstates corresponding to $E_{n,m}$ take the form

$$|\Psi_{n,m}\rangle \equiv |n\rangle|\phi_{n,m}\rangle, \tag{12}$$

where the mechanical wavefunctions $\phi_{n,m}(x) = \langle x|\phi_{n,m}\rangle$ are expressible in terms of Hermite functions centered at $x = \bar{x}_n$ (details not shown). The following eigenstate properties are easily verified:

$$\langle\hat{x}\rangle_{nm} \equiv \langle\Psi_{n,m}|\hat{x}|\Psi_{n,m}\rangle = \bar{x}_n, \tag{13}$$

$$\Delta x^2_{nm} \equiv \langle\Psi_{n,m}|(\hat{x} - \langle\hat{x}\rangle_{nm})^2|\Psi_{n,m}\rangle = \frac{m + 1/2}{2\Omega_n}. \tag{14}$$

In light of the above discussion we gain the following intuition about the structure of the Hamiltonian eigenstates in Eq. (12): the mechanical wavefunctions $\phi_{n,m}(x)$ are pushed further away from the fixed mirror as the photon number n is increased, while at the same time they become more and more squeezed in position. Such behaviour is schematised in Fig. 2.

Approach 2: standard quadratic expansion. Our second approach consists in a more traditional second-order expansion of Eq. (2). Specifically, we expand

$$\omega(x) \simeq \omega_0 - Gx + \frac{1}{2}\beta^2 x^2, \tag{15}$$

where $\beta^2 = 2\omega_0/L^2 = 2G^2/\omega_0$. For brevity, we shall refer to the resulting Hamiltonian as the *quadratic model*:

$$H_{\text{quad}} = \left(\omega_0 - G\hat{x} + \frac{1}{2}\beta^2\hat{x}^2\right)\left(\hat{a}^\dagger\hat{a} + \frac{1}{2}\right) + \frac{\hat{p}^2}{2} + \frac{1}{2}\Omega^2\hat{x}^2. \tag{16}$$

While the 'quadratic coupling' has been studied before in optomechanics[25–28], the focus has often been on the striking differences between a purely linear ($\beta = 0$) and a purely quadratic ($G = 0$) interaction. Here, on the other hand, our primary goal is to improve the accuracy of our Hamiltonian model: we want to explore the corrections to the linear model due to the higher order β term. This is in a similar spirit to ref.[14], where it was argued that the inclusion of higher order terms is necessary to investigate Planck-scale modifications to the canonical commutator. Taking Eq. (16) as a starting point, the relevant calculations for the quadratic model follow closely those of Sec 3.1, *mutatis mutandis*. What is more, we can here obtain compact analytical expressions. Specifically, we may recast the Hamiltonian in the form (7), with parameters

$$\Omega_n^2 = \Omega^2 + \left(n + \frac{1}{2}\right)\beta^2, \tag{17}$$

$$\bar{x}_n = \frac{G(n+1/2)}{\Omega_n^2}, \tag{18}$$

so that the resulting energy eigenvalues read

$$E_{n,m} = \left(n+\frac{1}{2}\right)\omega_0 + \Omega_n\left(m+\frac{1}{2}\right) - \frac{G^2(n+1/2)^2}{2\Omega_n^2}, \tag{19}$$

valid for all semipositive integers n, m. Also here we shall discuss the limit $n\to\infty$ as a matter of mathematical curiosity. Note that the quadratic model predicts a finite average mechanical displacement even in the limit of large n, while the mechanical frequencies are divergent with asymptotic scaling $\Omega_n \propto \sqrt{n}$, in turn implying that the mechanical wavefunctions become infinitely squeezed in position:

$$\lim_{n\to\infty} \langle \hat{x} \rangle_{nm} = \lim_{n\to\infty} \bar{x}_n = \frac{G}{\beta^2}, \tag{20}$$

$$\lim_{n\to\infty} \Omega_n = +\infty, \tag{21}$$

$$\lim_{n\to\infty} \Delta x_{nm} = 0. \tag{22}$$

Microscopic Approach

In this section we take as a starting point the microscopic Hamiltonian derived by C. K. Law through canonical quantization of a Fabry-Perot cavity with a movable mirror[15]. For the sake of numerical tractability we shall assume that only two degrees of freedom, one optical and one mechanical, are sufficient to model our optomechanical system. More precisely: we shall retain only one optical degree of freedom in Eq. (3.5) from ref.[15]. Furthermore, we shall not perform the gauge-like transformation used in Section IV of the same paper: the latter is a useful theoretical tool at first order in the coupling, but does not easily generalise to include the higher order effects we are trying to capture. Under the described assumptions, the Law Hamiltonian simplifies to

$$H_{\rm mic} = \frac{\hat{\Pi}^2}{2} + \frac{1}{2}\omega^2(\hat{x})\hat{Q}^2 + \frac{\hat{p}^2}{2} + \frac{1}{2}\Omega^2\hat{x}^2, \tag{23}$$

where $\hat{Q}$, $\hat{\Pi}$ are canonical quadrature operators for the cavity field mode and $\omega(\hat{x})$ retains the same form as before. The elementary canonical commutator for the cavity field is now $[\hat{Q}, \hat{\Pi}] = i$, and again all field operators commute with the mechanical variables $\hat{x}$ and $\hat{p}$. Note that Hamiltonian (23) leads to the Heinseberg equation $\frac{d}{dt}\hat{p} = -\Omega^2\hat{x} - \omega'(\hat{x})\omega(\hat{x})\hat{Q}^2$, i.e., the instantaneous radiation pressure force is proportional to the intensity of a single field quadrature (rather than to the field energy). This makes sense: since the (transverse) electric field $\boldsymbol{E}$ must vanish on the mirror, the radiation pressure force will be proportional to the squared magnetic field $|\boldsymbol{B}|^2$ alone (evaluated at the mirror surface). For completeness, the remaining equations of motion are $\frac{d}{dt}\hat{q} = \hat{p}$, $\frac{d}{dt}\hat{Q} = \hat{\Pi}$, $\frac{d}{dt}\hat{\Pi} = -\omega(\hat{x})^2\hat{Q}$, where the last two equations may be seen as an approximate reformulation of the wave equation for a single-mode cavity field of frequency $\omega(\hat{x})$. Hence, within the two-mode approximation, we argue that Eq. (23) should be a more reliable description of radiation pressure physics than Hamiltonian (2). In the next section, Eq. (23) will play the role of benchmark, or "true model", against which our various approximations shall be assessed. In the present section, we instead discuss the corrections to the linear model that arise in this framework, highlighting the issues that were not present in the phenomenological approach. In passing we remark that a microscopic Hamiltonian, alternative to that of C. K. Law, has been recently proposed for optomechanics[29]. In future studies, our analysis could be generalised to deal with this alternative theory, and/or to quantitatively assess the robustness of the two-mode approximation that we are currently taking for granted. Note that Hamiltonian (25) does not yield photon number conservation in general. More precisely, the concept of photon itself relies on identifying a reference frequency, for which a natural choice is $\omega_0 \equiv \omega(0)$. We then choose the following definition for the cavity annihilation operator:

$$\hat{a} = \sqrt{\frac{\omega_0}{2}}\hat{Q} + \frac{i}{\sqrt{2\omega_0}}\hat{\Pi}. \tag{24}$$

With the above definition, the annihilation operator $\hat{a}$ commutes with all mirror operators. This allows us to represent the pairs $(\hat{x}, \hat{p})$ and $(\hat{a}, \hat{a}^\dagger)$ in different Hilbert spaces, as is done for the phenomenological models of Sec 3. We found this approach convenient to set-up numerical calculations based on the truncation of Fock spaces. In passing we note that this was not the path taken in the seminal paper by C. K. Law[15], where instead $\hat{x}$– dependent annihilation operators were introduced to describe the cavity field. Hamiltonian (23) may be recast as

$$H_{\rm mic} = \nu(\hat{x})\left(\hat{a}^\dagger\hat{a} + \frac{1}{2}\right) + \frac{\lambda(\hat{x})}{2}(\hat{a}^2 + \hat{a}^{\dagger 2}) + \frac{\hat{p}^2}{2} + \frac{1}{2}\Omega^2\hat{x}^2, \tag{25}$$

where $\nu(\hat{x}) = (\omega(\hat{x})^2 + \omega_0^2)/2\omega_0$, $\lambda(\hat{x}) = (\omega(\hat{x})^2 - \omega_0^2)/2\omega_0$ and the cavity photon number $\hat{a}^\dagger\hat{a}$ is evidently not conserved due to the appearance of counter-rotating terms (i.e. $\hat{a}^2 + \hat{a}^{\dagger 2}$). Let us now discuss how to approximate Hamiltonian (23) at first and second order in the coupling G. A straightforward first-order expansion of Eq. (25) yields

$$H_{\rm mic}^{(1)} = H_{\rm lin} - \frac{G\hat{x}}{2}(\hat{a}^2 + \hat{a}^{\dagger 2}) \simeq H_{\rm lin}, \tag{26}$$

where the linear model (1) has been recovered through a rotating-wave approximation, justifiable in the parameter regime $\omega_0 \gg \Omega \gg g_0$ that we are considering here. More in detail, a back-of-the-envelope calculation shows that the counter-rotating terms only provide a contribution at order $O(G^2\hat{x}^2/\omega_0)$ – for example this can be proved by time-averaging the Hamiltonian on timescales $\gg 1/\omega_0$[30]. In the parameter regimes of interest we can thus reach the reassuring conclusion that the microscopic and phenomenological approaches yield the same linear model. We should however point out that there can be situations where ω_0 and Ω have comparable magnitude, and in that case the $(\hat{a}^2 + \hat{a}^{\dagger 2})$ term cannot be neglected even at first order in G[24].

It is at second order in G that non-negligible discrepancies arise between the microscopic and phenomenological approaches. Following similar lines of reasoning as above, we find that the second-order microscopic Hamiltonian is

$$H_{\rm mic}^{(2)} = H_{\rm quad} + \frac{\beta^2\hat{x}^2}{4}\left(\hat{a}^\dagger\hat{a} + \frac{1}{2}\right) - \frac{G\hat{x}}{2}(\hat{a}^2 + \hat{a}^{\dagger 2}), \tag{27}$$

where we recall $\beta^2 = 2\omega_0/L^2 = 2G^2/\omega_0$, and we note two additional terms that were not present in the phenomenological model and cannot be neglected at the considered order. Due to the counter-rotating terms, Hamiltonian (27) presents the same computational challenges as the original model in Eq. (23) – albeit its numerical solution appears to be slightly faster in the examples we explored. The relevance of Eq. (27) to our discussion is more conceptual than practical: it highlights that the phenomenological approach of the Section: Phenomenological Approach, when taken beyond first order in G, may begin to miss some of the finer details of optomechanical physics. In particular, the appearance of counter-rotating terms provides a *qualitative* departure from the phenomenological model.

Luckily, the examples to follow indicate that the analytical models derived via the phenomenological approach may still provide significant improvements to the linear model in the regime $\omega_0 \gg \Omega \gg g_0$ which is relevant to many experiments. Indeed, it can be shown that the corrections to $H_{\rm quad}$ appearing in Eq. (27) cancel each other out *on average* over timescales $\gg 1/\omega_0$ – see[30] for details on the time-averaging procedure. This may explain why the quadratic model (16) does improve the linear model, even though it does not fully capture all second order effects.

Numerical Examples

So far we have introduced several Hamiltonians that aim to improve the linear model. It is now interesting to compare these refined models in a concrete example: first by examining a few observables that characterize their low-energy eigensystems, then by looking at their predictions for the time evolution of mirror position and field amplitude. Since we are considering small deviations from the predictions of $H_{\rm lin}$, it is practically impossible to compare by eye the plots of absolute quantities. Instead, for any quantity A calculated via a given approximate model, we shall plot the absolute error $|A - A_{\rm mic}|$, where $A_{\rm mic}$ is computed by solving $H_{\rm mic}$ numerically. Note that numerical solutions are adopted also for $H_{\rm phen}$ and $H_{\rm mic}^{(2)}$. For all these cases we wrote a simple Mathematica script to diagonalize the Hamiltonian in a truncated space and hence calculate all quantities of interest. To confirm the solidity of these results we performed the time-evolution calculations (Fig. 4) also in Python, which resulted in visually identical plots. For our purposes truncations of $n_{\rm max} = 20$ photons and $m_{\rm max} = 30$ phonons were sufficient to obtain convergence: our plots did not show visible changes when considering nearby truncation numbers of $n_{\rm max} + 1$ and $m_{\rm max} + 1$. Yet, note that these numbers rely heavily on the chosen model parameters, and on the number of reliable eigenvalues one is seeking to obtain.

In the displayed examples we set $\Omega = 100 g_0$, inspired by recent experiments featuring $g_0/\Omega \lesssim 0.01$[2–4], while the bare cavity frequency is fixed at $\omega_0 = 100\Omega$. Qualitatively similar results were obtained by increasing ω_0 to $10^3\Omega$. With our current numerical means we found it difficult to obtain reliable results when increasing ω_0 further: the handling of such cases required prohibitively high numerical precisions. It may be useful to overcome this limitation in the future, in order to address systems where many orders of magnitude separate mechanical and optical frequencies.

Low-energy eigensystems. To compare eigensystems, we focus on the following quantities that depend on the photon number n:

(i) Lowest energy eigenvalue, $E_{n,0}$
(ii) Average mechanical displacement, $\langle\hat{x}\rangle_{n,0}$
(iii) Mechanical uncertainty, $\Delta x_{n,0}$

Note that the eigensystems of Hamiltonians $H_{\rm lin}$, $H_{\rm phen}^{(2)}$, $H_{\hat{n}}$ are *fully characterized* by these quantities. In contrast, n is not a good quantum number for $H_{\rm mic}$ and $H_{\rm mic}^{(2)}$, since these Hamiltonians do not commute with $\hat{n}$. Yet, in the parameter regimes here considered we were able define an effective photon number n as the integer

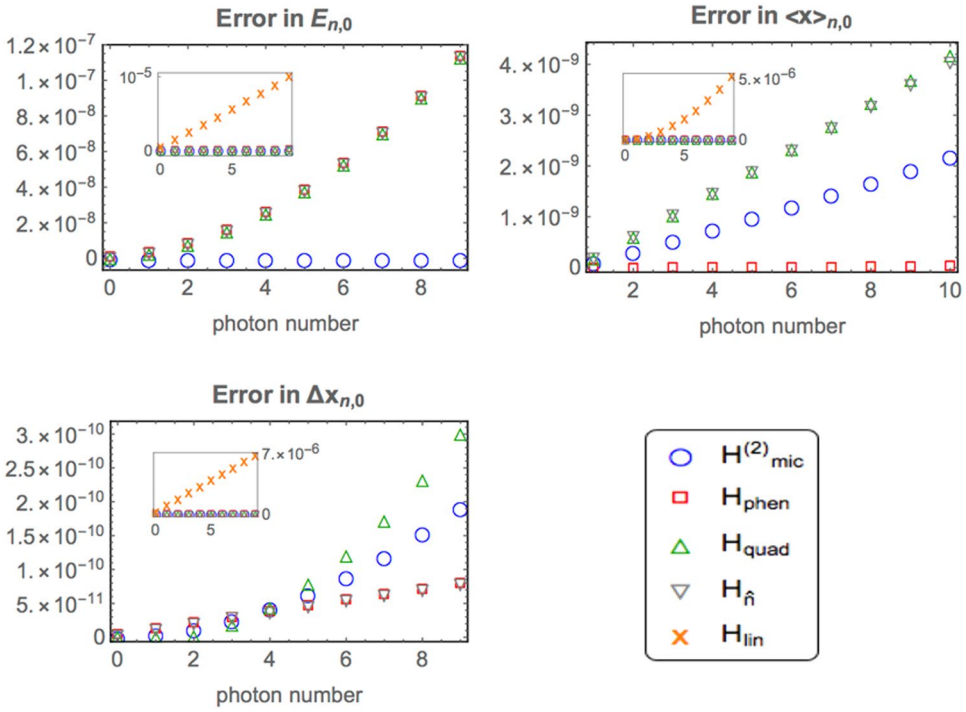

Figure 3. Performance of the various Hamiltonians in predicting the low-energy eigensystem properties of a two-mode optomechanical system. The microscopic model $H_{\rm mic}$ is taken as benchmark (or "true model"). For these plots we consider a Fabry-Perot optomechanical setup with parameters $\omega_0 = 10^2\Omega$, $\Omega = 10^2 g_0$. Energies are measured in units such that $\Omega = 1$, while lengths ($\langle\hat{x}\rangle_{n,0}$, $\Delta x_{n,0}$) are measured in units of the zero-point width $x_{zpf} = 1/\sqrt{2\Omega}$. Errors relative to the linear model are shown in insets due to their different scale.

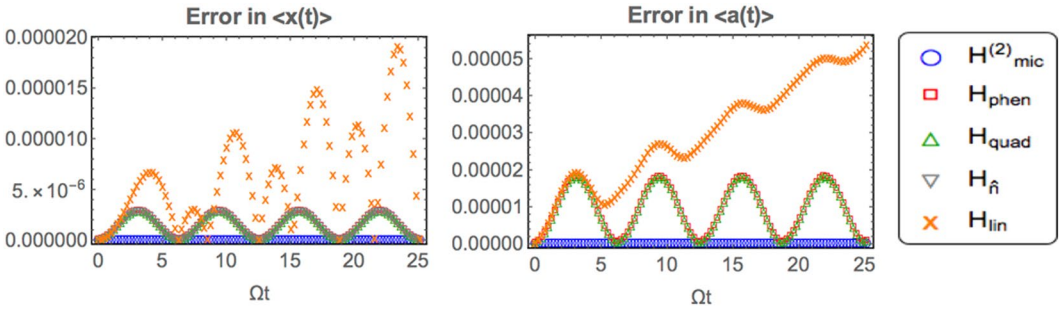

Figure 4. Performance of the different models in predicting low-energy dynamics in the system. As in Fig. 3, we consider parameters $\omega_0 = 10^2\Omega$, $\Omega = 10^2 g_0$. The dynamics of $\langle\hat{a}\rangle$ and $\langle\hat{x}\rangle$ are calculated for the initial state (28) with $\alpha = 2$. While $\langle\hat{a}(t)\rangle$ is dimensionless, $\langle\hat{x}(t)\rangle$ is measured in units of the zero-point width $x_{zpf} = 1/\sqrt{2\Omega}$.

closest to $\bar{n} = \langle\hat{a}^\dagger\hat{a}\rangle$, since $|n - \bar{n}|$ remained small in all the reported examples (while n is obviously an integer, note that $\bar{n}$ may not be so in a non-number-conserving Hamiltonian). In turn, this allowed us to identify the lowest eigenvalue at fixed n, $E_{n,0}$, as well as the associated eigenstate $|\Psi_{n,0}\rangle$. From these we were able to define, and calculate, quantities (i)–(iii) for the models $H_{\rm mic}$ and $H^{(2)}_{\rm mic}$. Figure 3 shows that all the approaches considered here provide a significant improvement to the linear model, but at this stage there is no clear winner: while $H^{(2)}_{\rm mic}$ is better at predicting energy eigenvalues, the phenomenological Hamiltonian $H_{\rm phen}$ can predict mechanical equilibrium positions and (most) variances more accurately. This suggests that it may be worth keeping all these Hamiltonians in one's theoretical toolbox for the sake of future optomechanical studies. In passing, it is interesting to note that $H_{\hat{n}}$ can be seen as a sort of hybrid model emulating properties of both $H_{\rm quad}$ (equilibrium positions) and $H_{\rm phen}$ (mechanical variances).

Dynamics. To compare dynamical predictions we take the initial state

$$|\Psi(0)\rangle = |\alpha\rangle_a|0\rangle_b, \tag{28}$$

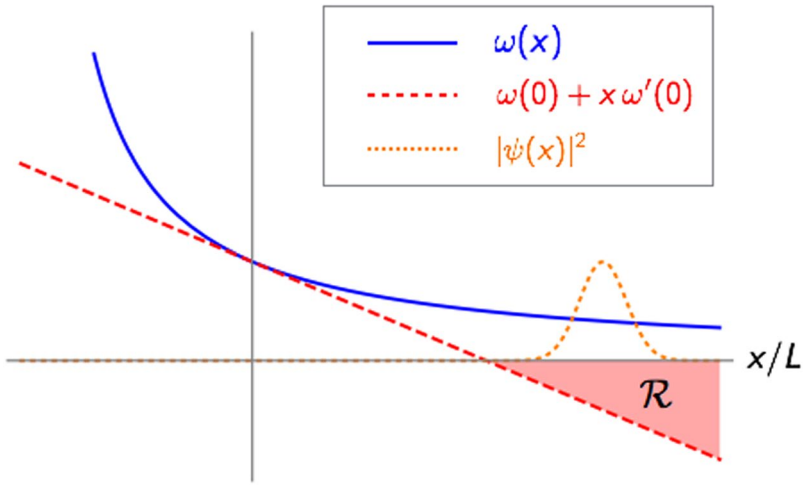

Figure 5. An illustration of the pathology carried by the linear model. While a well-defined optomechanical model features $\omega(x) > 0$ for all x (blue continuous curve), the linearization of $\omega(x)$ (red-dashed curve) produces a non-physical region (R) where the cavity frequency is negative. It then possible to construct states of arbitrarily low energy by concentrating the mechanical probability density (orange dotted line) in the region R, and subsequently populating the cavity with a large number of photons.

where $|\alpha\rangle_a = e^{-|\alpha|^2/2}\sum_n(\alpha^n/n!)|n\rangle_a$ is a coherent state and $|0\rangle_b$ is the bare ground state of the mechanics. It is apparent that the evolution of initial state (28) is going to involve several photon number sectors even with the number-conserving Hamiltonians. Moreover, according to the linear model, the evolution of this state can induce interesting nonclassical features in the system, such as Wigner-Function negativity and opto-mechanical entanglement[20]. Therefore, we think that the initial state (28) embodies an interesting test-bed for our various approximate Hamiltonians: a reliable description of the subsequent dynamics must capture well the evolution of self-correlations in the cavity field together with entanglement between the two subsystems. In our examples we picked $\alpha = 2$, and looked at the accuracy of the various models in predicting the time-dependent averages $\langle\hat{x}(t)\rangle$ and $\langle\hat{a}(t)\rangle$: the relevant results are displayed in Fig. 4. From these we infer that $H^{(2)}_{\rm mic}$ has an edge on the other models, as it may be expected from its construction as the 'correct' second-order expansion of $H_{\rm mic}$. As a corollary, we deduce that the inclusion of counter-rotating terms will eventually become necessary in trying to model optomechanical system with ever higher accuracy. On the other hand, the good news is that once again the phenomenological approach provides a significant improvement to the linear model (except for a few isolated points in time, where the linear model yields better estimates for $\langle\hat{x}(t)\rangle$). Furthermore, in the chosen example we do not observe significant differences between the dynamical predictions of $H_{\rm phen}$, $H_{\hat{n}}$ and $H_{\rm quad}$. Under these circumstances, our choice of model for further analysis would naturally fall on $H_{\rm quad}$ due to its simple analytical solution.

Conclusions and Outlook

We have proposed and compared several Hamiltonians that go beyond the linear model of optomechanics, featuring corrections that are either phenomenologically or microscopically derived. Using a two-mode truncation of Law's Hamiltonian[15] as our benchmark, we were able to confirm that the phenomenological approach, common in the literature, is able to provide meaningful corrections to the linear model. A particularly reassuring observation is that, in the regime $\omega \gg \Omega \gg g_0$ studied here, these corrections are well captured by the analytically solvable model $H_{\rm quad}$, i.e., a straightforward second-order expansion of the phenomenological Hamiltonian (2). However, we also pointed out that the phenomenological approach does not fully capture all second order corrections arising from a microscopic treatment of radiation pressure. In particular we have outlined an important effect, the breakdown of photon number conservation, which can provide non-negligible corrections even in parameter regimes where dynamical-Casimir effects are usually discounted.

Our work may benefit future experiments probing the single-photon strong coupling regime or aiming for high-precision optomechnical measurements. More importantly, it opens a discussion that may uncover new avenues for the theoretical modelling of optomechanics, beyond the domain of applicability of the linear model. There are several important questions that our work leaves open and that should be addressed in future studies. First, our analysis is confined to a two-mode scenario. In the quest for strong coupling and/or high precision modelling, a multi-mode treatment[31] (including several degrees of freedom for both light and mechanics) may eventually become necessary. Second, we have left system-environment interactions out of our discussion. Due to the presence of three very different energy scales (ω_0, Ω, g_0), we anticipate that it will be challenging to develop an accurate open-system model for optomechanics that goes beyond the existing phenomenological treatments. Yet, identifying a reliable Hamiltonian is a crucial first step towards the rigorous modelling of an open quantum system[32]. Third, we have assumed the bare mechanical potential to be harmonic. Depending on the implementation, anharmonicity in the mirror potential[33] may provide new corrections that can be qualitatively different from those studied here. Finally, a model including relativistic corrections may be eventually needed. The theoretical

challenge will increase significantly in trying to address any of these limitations of our work, yet it will be a worthwhile pursuit in the quest to model ever more sophisticated optomechanics experiments.

Availability of materials and data. The original Mathematica and Phython codes utilised to produce the plots in Fig. 3 are available upon request.

Appendix A: Negative energies in the linear model. In this section we shed further light on the pathologies of the linear model of optomechanics, which to the best of our knowledge were first outlined by[23]. We first take one step back and consider a generic optomechanical Hamiltonian of the form

$$H = \omega(\hat{x})\left(\hat{a}^\dagger\hat{a} + \frac{1}{2}\right) + \frac{\hat{p}^2}{2} + V(\hat{x}), \tag{29}$$

where both the frequency dependence of ω and the mechanical potential V can be left generic at this stage. We will only assume that V is a regular function, so that it cannot encode hard-wall boundary conditions (more on this point below). It is easy to show that, if there is a region for x where $\omega(x) < 0$, the Hamiltonian cannot be lower-bounded. Indeed, let us suppose that $\omega(x)$ is not everywhere positive, and that there is a ground state with finite energy E_0. For any quantum state it would then follow $E_0 \leq \langle H\rangle$. In particular let us consider a product state $|n\rangle|\psi\rangle \equiv |n\rangle_a \otimes |\psi\rangle_b$, where $|n\rangle_a$ indicates a fock state of the cavity field, while $|\psi\rangle_b$ is a generic mechanical wavefunction. Taking the expectation value of H we obtain

$$E_0 \leq \left(n + \frac{1}{2}\right)\langle\psi|\omega(\hat{x})|\psi\rangle + \langle\psi|\left(\frac{\hat{p}^2}{2} + V(\hat{x})\right)|\psi\rangle. \tag{30}$$

If the cavity frequency can assume negative values in a certain region $\mathcal{R} \equiv \{x|\omega(x) < 0\}$, it is always possible to obtain $\langle\psi|\omega(\hat{x})|\psi\rangle < 0$, for example by choosing $\psi(x) \equiv \langle x|\psi\rangle$ as a smooth function with support in $\mathcal{R}$ (See Fig. 5). At the same time, the second term on the right-hand side (RHS) of Eq. (30) is a finite constant if the potential does not display singularities. It follows that the expression on the RHS tends to $-\infty$ when $n \to \infty$, so that E_0 cannot be finite.

In hindsight this result may appear obvious, as the very concept of a single-mode cavity implicitly assumes $\omega(x) > 0$. Yet, the common linear approximation $\omega(x) \simeq \omega_0 - Gx$ fails to satisfy this requirement. Note that in the above discussion we did not need to specify the functional form of V, hence we can conclude that the outlined pathology cannot be cured by adding anharmonic terms to the mechanical confining potential. The only way to retain a linearised $\omega(x)$, while also ensuring that H in Eq. (29) is lower bounded, is to impose hard-wall boundary conditions on the oscillator, so that all mechanical wavefunctions are forced to vanish in the region $\mathcal{R}$.

References

1. Bowen, W. P. & Milburn, G. J. Quantum optomechanics, CRC Press (2015).
2. Aspelmeyer, M., Kippenberg, T. J. & Marquardt, F. Cavity optomechanics. *Reviews of Modern Physics* **86**, 1391 (2014).
3. Marquardt, F. Optomechanics: Push towards the quantum limit. *Nature Physics* **4**, 513 (2008).
4. Kippenberg, T. J. & Vahala, K. J. Cavity Optomechanics: Back-Action at the Mesoscale. *Science* **321**, 1172 (2008).
5. Cleland, A. Optomechanics: Photons refrigerating phonons. *Nature Physics* **5**, 458 (2009).
6. Gröblacher, S., Hammerer, K., Vanner, M. R. & Aspelmeyer, M. Observation of strong coupling between a micromechanical resonator and an optical cavity field. *Nature* **460**, 724 (2009).
7. Paternostro, M. Engineering Nonclassicality in a Mechanical System through Photon Subtraction. *Physical Review Letters* **106**, 183601 (2011).
8. Vanner, M. R. *et al*. Pulsed quantum optomechanics. *Proc. Natl. Acad. Sci. USA* **108**, 16182 (2011).
9. Fabre, C. *et al*. Quantum-noise reduction using a cavity with a movable mirror. *Physical Review A* **49**, 1337 (1994).
10. Mancini, S. & Tombesi, P. Quantum noise reduction by radiation pressure. *Physical Review A* **49**, 4055 (1994).
11. Aldana, S., Bruder, C. & Nunnenkamp, A. Equivalence between an optomechanical system and a Kerr medium. *Physical Review A* **88**, 043826 (2013).
12. Rabl, P. Photon Blockade Effect in Optomechanical Systems. *Physical Review Letters* **107**, 063601 (2011).
13. Pikovski, I., Vanner, M. R. Aspelmeyer, M., Kim, M. S. & Brukner, Ĉ. Probing Planck-scale physics with quantum optics. *Nature Physics* **8**, 39339 (2012).
14. Kumar, S. P. & Plenio, M. B. Experimentally feasible quantum optical tests of Planck-scale physics, arXiv:1708.05659.
15. Law, C. K. Interaction between a moving mirror and radiation pressure: A Hamiltonian formulation. *Physical Review A* **51**, 2537 (1995).
16. Nunnenkamp, A., Borkje, K. & Girvin, S. M. Single-Photon Optomechanics. *Physical Review Letters* **107**, 063602 (2011).
17. Rimberg, A. J., Blencowe, M. P., Armour, A. D. & Nation, P. D. A cavity-Cooper pair transistor scheme for investigating quantum optomechanics in the ultra-strong coupling regime. *New Journal of Physics* **16**, 055008 (2014).
18. Leijssen, R., La Gala, G., Freisem, L., Muhonen, J. T. & Verhagen, E. Nonlinear cavity optomechanics with nanomechanical thermal fluctuations. *Nature Communications* **8**, 16024 (2017).
19. Ludwig, M., Kubala, B. & Marquardt, F. The optomechanical instability in the quantum regime. *New Journal of Physics* **10**, 095013 (2008).
20. Bose, S., Jacobs, K. & Knight, P. L. Preparation of nonclassical states in cavities with a moving mirror. *Physical Review A* **56**, 4175 (1997).
21. Mancini, S., Man'ko, V. I. & Tombesi, P. Ponderomotive control of quantum macroscopic coherence. *Physical Review A* **55**, 3042 (1997).
22. Latmiral, L. & Mintert, F. Deterministic preparation of highly non-classical quantum states of massive oscillators, arXiv:1705.10334.
23. Brunelli, M., Xuereb, A., Ferraro, A., De Chiara, G., Kiesel, N. & Paternostro, M. Out-of-equilibrium thermodynamics of quantum optomechanical systems. *New Journal of Physics* **17**, 035016 (2015).
24. Macrì, V., Ridolfo, A., Di Stefano, O., Kockum, A. F., Nori, F. & Savasta, S. Nonperturbative Dynamical Casimir Effect in Optomechanical Systems: Vacuum Casimir-Rabi Splittings. *Physical Review X* **8**, 011031 (2018).

25. Jayich, A. M. *et al*. Dispersive optomechanics: a membrane inside a cavity. *New Journal of Physics* **10**, 095008 (2008).
26. Sankey, J. C. *et al*. Strong and tunable nonlinear optomechanical coupling in a low-loss system. *Nature Physics* **6**, 707 (2010).
27. Nunnenkamp, A., Borkje, K., Harris, J. G. E. & Girvin, S. M. Cooling and squeezing via quadratic optomechanical coupling. *Physical Review A* **82**, 021806(R) (2010).
28. Liao, J.-Q. & Nori, F. Single-photon quadratic optomechanics. *Scientific Reports* **4**, 6302 (2014).
29. Khorasani, S. Higher-Order Interactions in Quantum Optomechanics: Revisiting Theoretical. *Foundations, Applied Sciences* **7**, 656 (2017).
30. James, D. F. & Jerke, J. Effective Hamiltonian theory and its applications in quantum information. *Canadian Journal of Physics* **85**, 625 (2007).
31. Cheung, H. K. & Law, C. K. Nonadiabatic optomechanical Hamiltonian of a moving dielectric membrane in a cavity. *Physical Review A* **84**, 023812 (2011).
32. Breuer, H. P. & Petruccione, F. *The theory of open quantum systems,* Oxford University Press (2002).
33. Latmiral, L., Armata, F., Genoni, M. G., Pikovski, I. & Kim, M. S. Probing anharmonicity of a quantum oscillator in an optomechanical cavity. *Physical Review A* **93**, 052306 (2016).

Acknowledgements

We acknowledge fruitful discussions with G. Adesso,, A. Armour, S. Bose, L.A.C. Correa, A. Ferraro, M.G. Genoni, O. Hess, M.S. Kim, S.P. Kumar, G.J. Milburn, F. Mintert, A. Nunnenkamp, M. Paternostro, M. Plenio, A. Serafini, H. Ulbricht and especially Federico Armata and Daniele Dorigoni. T.T. acknowledges financial support from the Foundational Questions Institute (Grant No. FQXi-RFP-1601), and from the University of Nottingham via a Nottingham Research Fellowship. K.S. acknowledges financial support from the University of Nottingham through a Dr Margaret Jackson Summer Bursary Award.

Author Contributions

T.T. planned the research. K.S. performed the analytical calculations of Section: Phenomenological Approach and produced the associated Mathematica codes, T.T. worked on the microscopic model of Section: Microscopic approach and produced the associated codes. Both authors contributed equally to the discussion of results, the writing of the manuscript and the production of figures.

Additional Information

Competing Interests: The authors declare no competing interests.

Publisher's note: Springer Nature remains neutral with regard to jurisdictional claims in published maps and institutional affiliations.